
video-SALMONN 2: Captioning-Enhanced Audio-Visual Large Language Models

**Changli Tang¹*, Yixuan Li¹*, Yudong Yang¹, Jimin Zhuang¹, Guangzhi Sun²,
Wei Li³, Zejun Ma³, Chao Zhang^{1†}**

Tsinghua University¹, University of Cambridge², ByteDance³
 {tcl24, yixuan-121}@mails.tsinghua.edu.cn, cz277@tsinghua.edu.cn

Abstract

Videos contain a wealth of information, and generating detailed and accurate descriptions in natural language is a key aspect of video understanding. In this paper, we present video-SALMONN 2, an advanced audio-visual large language model (LLM) with low-rank adaptation (LoRA) designed for enhanced video (with paired audio) captioning through directed preference optimisation (DPO). We propose new metrics to evaluate the completeness and accuracy of video descriptions, which are optimised using DPO. To further improve training, we propose a novel multi-round DPO (MrDPO) approach, which involves periodically updating the DPO reference model, merging and re-initialising the LoRA module as a proxy for parameter updates after each training round (1,000 steps), and incorporating guidance from ground-truth video captions to stabilise the process. Experimental results show that MrDPO significantly enhances video-SALMONN 2’s captioning accuracy, reducing the captioning error rates by 28%. The final video-SALMONN 2 model, with just 7 billion parameters, surpasses leading models such as GPT-4o and Gemini-1.5-Pro in video captioning tasks, while maintaining highly competitive performance to the state-of-the-art on widely used video question-answering benchmarks among models of similar size. Codes are available at <https://github.com/bytedance/video-SALMONN-2>.

1 Introduction

Large language models (LLMs) have exhibited outstanding capabilities in a wide range of natural language processing tasks, and in some instances, have even approached human-level performance [1–6]. LLMs’ remarkable ability to understand, generate, and reason with text has sparked widespread interest among researchers, attracting both academia and industry to extend them to multimodal understanding and generation. To endow LLMs with multimodal understanding capability, recent studies adopted a paradigm of training modality adapters and aligners between multimodal encoders and LLMs. This approach leverages world knowledge in the textual LLM to interpret diverse types of data perceived by multimodal encoders, enabling the generation of meaningful insights. Over the past two years, many multimodal LLMs have emerged following this paradigm across different modalities. These include models for image and silent video understanding [7–19], audio understanding [20–27], and audio-visual understanding [28–34].

Text descriptions paired with data are essential for building effective multimodal large language models (LLMs). This is because most contemporary multimodal LLMs treat captioning as a cornerstone task during pre-training or supervised fine-tuning (SFT), aligning the output space of multimodal encoders with the input space of textual LLM backbones. Such alignment enables the models to

*Equal contribution

†Corresponding author

recognise and understand events in multimodal data. Therefore, collecting high-quality, detailed, and low-hallucination text descriptions aligned with multimodal inputs is crucial for enhancing the model’s multimodal understanding and reasoning capabilities. In the context of video understanding, generating accurate and comprehensive captions remains a significant challenge. Videos encode complex content that spans both spatial features within individual frames and audio-visual events across temporal sequences. Despite the prevalence of incompleteness and hallucinations in video captions, few studies have addressed caption quality, largely due to the lack of reliable quantitative evaluation metrics and effective training methods. Moreover, although audio is typically paired with video and provides vital complementary information, most existing visual LLMs lack audio processing capabilities, further contributing to the deficiencies in existing video captioning systems.

In this paper, we introduce video-SALMONN 2, a multimodal LLM that supports both audio and visual inputs and primarily focuses on detailed and holistic audio-visual captioning. Building upon a pre-trained visual LLM, video-SALMONN 2 is further enhanced with auditory capabilities by training on audio-only data as well as videos with synchronised audio tracks. This enables the model to simultaneously “see” and “hear” the video, emulating the way humans perceive and interpret multimedia content. To accurately assess the performance of the model, new metrics to evaluate captioning quality are proposed, which then serve as the objective to optimise during reinforcement learning (RL) based on direct preference optimisation (DPO) [35]. A novel multi-round DPO (MrDPO) method is proposed and performed based on the preferences guided by the metrics. Experiments demonstrate that video-SALMONN 2 with 7 billion (B) parameters can generate detailed and accurate video captions and even outperforms much larger commercial models such as GPT-4o and Gemini-1.5-Pro, and it also maintains competitive performance to the open-source state-of-the-art (SOTA) multimodal LLMs of similar model size on commonly used video question-answering (QA) benchmarks. Our main contributions can be summarised as follows:

- We develop video-SALMONN 2, a powerful audio-visual LLM that generates high-quality video captions, outperforming larger commercial models such as GPT-4o and Gemini-1.5 in terms of completeness and accuracy.
- We introduce an evaluation pipeline that computes the missing and hallucination rates of audio-visual events in video captions using text-based LLMs, breaking down the process into sub-tasks suited for current LLMs. Additionally, we provide a new benchmark for video captioning with a human-annotated test set.
- We propose the MrDPO approach to optimise multimodal LLMs for video captioning, incorporating periodic updates to the DPO reference model, merging and reinitialising the low-rank adaptation (LoRA) [36] proxy, and smoothing the training loss using SFT based on ground-truth captions.

2 Related Work

2.1 Multimodal LLMs

Following the paradigm of connecting multimodal encoders to LLMs using modality adapters, various models have been developed. For image-based LLMs, LLaVA [7, 8] applies instruction tuning [37] to enhance performance on zero-shot tasks. BLIP-2 [9] uses Q-Former to link a frozen encoder with an LLM, while VILA [11] explores pre-training strategies, achieving impressive results in video QA. InternVL [12] scales up the size of visual encoders for improved image representation. For silent video understanding, Video-LLaVA [13] aligns both image and video adapters to learn unified representations. ShareGPT4Video [14] uses GPT-4 to generate dense video captions, improving data quality, and LLaVA-Hound [38] introduces DPO to enhance video LLMs’ understanding capabilities. LLaVA-OneVision [15] enhances the performance of open multimodal LLMs in single-image, multi-image, and silent video scenarios and enables strong transfer learning from images to videos. LLaVA-Video [16] further creates a high-quality synthetic dataset to further push the performance boundary of video understanding. Qwen2-VL [39] and Qwen2.5-VL [17] transform images of varying resolutions into different numbers of tokens and design rotary position embedding to enhance video understanding. NVILA [40] further enhances the performance of video understanding through scaling up the spatial and temporal resolutions first and then compressing. AuroraCap [41] focuses on video captioning from different perspectives and achieves favourable results on its proposed VDC benchmark. F-16 [18] improves the performance of video LLMs through high-frame-rate modeling with dense sampling at 16 frames per second.

In the realm of audio perception, SALMONN [21] uses a dual-encoder structure and can perform zero-shot audio reasoning tasks. LTU [24] and LTU-AS [25] trained on a large audio event QA dataset can answer open-ended questions about audio content. Qwen-Audio [22] and Qwen2-Audio [23] are built on large amounts of audio data to achieve high performance on a wide range of carefully selected audio tasks. Other works [26, 27] extend the LLM to perceive spatial audio information obtained from microphone array recordings.

As the visual frame sequence is often paired with audio in real-world video recordings, some studies investigate understanding non-silent video. Vid2Seq [42] utilises speech transcriptions to enhance video captioning. video-SALMONN [30] uses a multi-resolution causal Q-Former to understand audio and video simultaneously. video-SALMONN-o1 [34] enhances audio-visual reasoning abilities through process DPO. The Google Gemini model achieves video understanding as a native multimodal LLM built upon text, audio, and visual tokens [28]. AVicuna [33] achieves audio-visual temporal understanding by introducing pseudo-untrimmed video data. Video-LLaMA [43] and Video-LLaMA 2 [29] directly concatenate audio and visual tokens for joint audio and video understanding. InternVideo2 [44] aligns video to audio events, speech and text through cross-modal contrastive learning for joint audio-video understanding. Qwen2.5-Omni [45] not only achieves audio-visual understanding but is also able to generate text and speech in a streaming manner.

2.2 RL for LLMs

RL with human feedback (RLHF) [46] is a widely adopted strategy for improving the performance of textual LLMs. Early approaches commonly employed proximal policy optimisation [47] in conjunction with a reward model trained on human preference data. Building on this foundation, DPO [35] eliminates the need for a separate reward model by leveraging the LLM itself to optimise directly from paired preference data. KTO [48] further simplifies the process by removing the requirement for paired preference data altogether. Extending this direction, RLAIF [49] adopts a cost-efficient framework by using model-generated feedback in place of human input, significantly reducing human involvement. Most recently, GRPO [50] improves efficiency and stability, particularly in tasks such as mathematical reasoning, by comparing relative rewards among candidate responses within a group, thereby removing the need for a separate value network.

3 Methods

3.1 Model Architecture

The overall architecture of our model is illustrated in Fig. 1. The paired sequences of audio and visual frames from each video are fed into the audio and visual encoders separately. Users can provide textual prompts to guide the model in performing specific tasks based on the video content. This structure is implemented by incorporating a separate audio encoder branch to a pre-trained visual LLM, which enables the model to process and understand paired audio-visual sequences without degrading its visual performance.

In this structure, audio and visual tokens are computed independently in their respective branches. For the visual branch, the input visual frame sequence is first downsampled at a fixed frame rate of ϕ frames/second, and the total number of frames to sample is $n = \phi T$, where T is the duration of the input video in seconds. Let m be the maximum number of frames to sample based on the resource constraint. If $n > m$, the frame rate is further reduced to $\phi' = \lfloor m/T \rfloor$, resulting in $n = \phi' T \leq m$. Let \mathbf{I}_i be the i th sampled visual frame, and each visual frame in $\mathbf{I}_1, \mathbf{I}_2, \dots, \mathbf{I}_n$ is transformed to visual tokens independently using a pre-trained visual encoder $\text{Encoder}_{\text{Visual}}$ followed by a visual modality aligner $\text{Aligner}_{\text{Visual}}$, as shown below:

$$\mathbf{H}_i^{\text{Visual}} = \text{Aligner}_{\text{Visual}}(\text{Encoder}_{\text{Visual}}(\mathbf{I}_i)), \quad 1 \leq i \leq n,$$

where $\mathbf{H}_i^{\text{Visual}}$ is the visual tokens corresponding to \mathbf{I}_i .

The audio frame sequence \mathbf{S} is fed into a pre-trained audio encoder $\text{Encoder}_{\text{Audio}}$. Since $\text{Encoder}_{\text{Audio}}$ may have a maximum processing duration t_{\max} , the audio will be sliced into $l = \lceil T/t_{\max} \rceil$ segments of t_{\max} -length and processed separately by $\text{Encoder}_{\text{Audio}}$ by

$$\mathbf{Z}_j^{\text{Audio}} = \text{Encoder}_{\text{Audio}}(\mathbf{S}_{(j-1) \times t_{\max}:j \times t_{\max}}), \quad 1 \leq j \leq l,$$

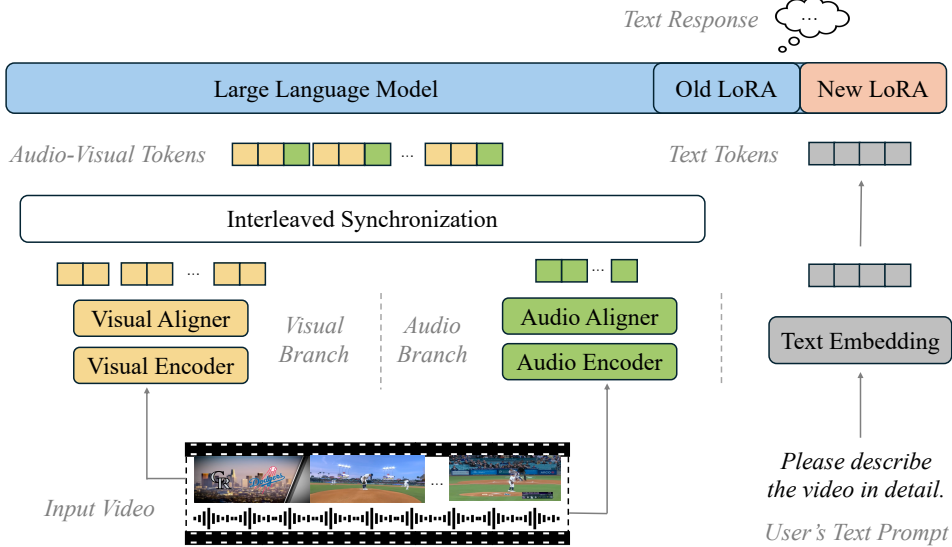


Figure 1: The architecture of video-SALMONN 2. The input video is processed by separate visual and audio branches, which extract visual and audio tokens from the corresponding frame sequences. These tokens are then synchronously interleaved and combined with tokens from the text prompt to form the input to the LLM backbone. During training, video-SALMONN 2 dynamically merges and reinitialises LoRA proxies, ensuring that only one LoRA proxy is active at any given time.

where $\mathbf{Z}_j^{\text{Audio}}$ is the audio feature vector output by the audio encoder of the j th audio segment.

As suggested by [51], a segment-level positional embedding is added before the modality aligner to improve the performance of long-form audio. Denote $\mathbf{Z}_j^{\text{Pos}}$ as the segment-level position embedding matrix corresponding to the position j , $\text{Concat}(\cdot)$ as the concatenation operation along the time dimension, and $\text{Aligner}_{\text{Audio}}$ as the audio modality aligner. The audio token sequence $\mathbf{H}^{\text{Audio}}$ for the whole audio can be computed as shown in Eqns. (1)–(3):

$$\tilde{\mathbf{Z}}_j^{\text{Audio}} = \mathbf{Z}_j^{\text{Audio}} + \mathbf{Z}_j^{\text{Pos}}, \quad 1 \leq j \leq l \quad (1)$$

$$\tilde{\mathbf{Z}}^{\text{Audio}} = \text{Concat}(\tilde{\mathbf{Z}}_1^{\text{Audio}}, \tilde{\mathbf{Z}}_2^{\text{Audio}}, \dots, \tilde{\mathbf{Z}}_l^{\text{Audio}}) \quad (2)$$

$$\mathbf{H}^{\text{Audio}} = \text{Aligner}_{\text{Audio}}(\tilde{\mathbf{Z}}^{\text{Audio}}). \quad (3)$$

Next, the audio and visual tokens are interleaved chronologically to form the input audio-visual token sequence \mathbf{H} fed into the LLM backbone, and \mathbf{H} is obtained based on Eqns. (4)–(6) by

$$\alpha_i = l \cdot i/n, \quad 1 \leq i \leq n \quad (4)$$

$$\mathbf{H}_i = \text{Concat}(\mathbf{H}_i^{\text{Visual}}, \mathbf{H}_{\alpha_{i-1}:\alpha_i}^{\text{Audio}}), \quad 1 \leq i \leq n \quad (5)$$

$$\mathbf{H} = \text{Concat}(\mathbf{H}_1, \mathbf{H}_2, \dots, \mathbf{H}_n). \quad (6)$$

Finally, the text-based backbone LLM is required to generate a text response $\hat{\mathbf{Y}}$ given the user's text prompt \mathbf{P} and the audio-visual token sequence \mathbf{H} :

$$\hat{\mathbf{Y}} = \arg \max_{\mathbf{Y}} P(\mathbf{Y}|\mathbf{P}, \mathbf{H}). \quad (7)$$

3.2 Training Strategies

To equip the visual LLM with audio perceptual capabilities, we adopt a multi-stage training strategy that enables effective utilisation of audio information for video understanding while preserving the model's visual processing performance. Starting from a well-trained visual LLM, the training pipeline consists of three stages: audio modality alignment, audio-visual SFT, and RL via the proposed MrDPO method. The backbone LLM, the visual encoder, and the audio encoder are kept frozen during training to prevent catastrophic forgetting.

Audio modality alignment extends the visual LLM by adding a parallel audio branch, enabling auditory perception abilities. During this stage, only the audio aligner is trained on a large audio

dataset, while the rest of the model remains frozen to preserve its original visual understanding performance. Speech recognition and audio captioning are used in the training with the cross-entropy loss function based on the reference speech transcriptions and audio captions.

Audio-visual SFT is applied after aligning the audio modality, utilising annotated video data to train the model for synchronised and integrated audio-visual understanding based on interleaved audio and visual token sequences. During this SFT stage, the model is optimised using cross-entropy loss, with video descriptions serving as ground-truth labels that encapsulate both audio and visual information. To further enhance the backbone LLM’s capability in processing paired audio-visual token sequences, a LoRA [36] adapter is used and jointly trained. Additionally, the audio aligner is trained to map the audio encoder’s output to the input representation space of the LLM, ensuring seamless interpretation of audio tokens by the backbone model.

RL based on MrDPO is applied after audio-visual SFT to address issues such as missing information and hallucinations. Further details are discussed in Section 3.3.

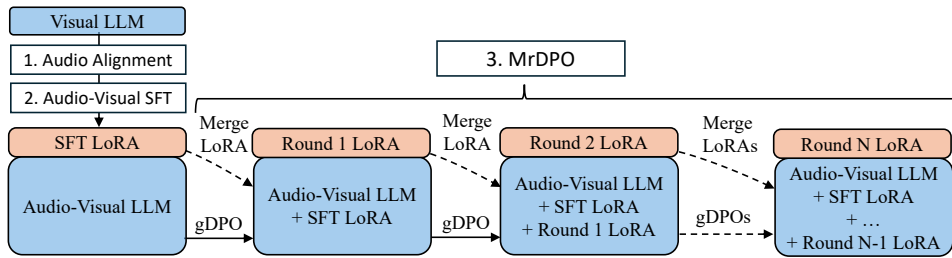


Figure 2: An overview of the training process including audio modality alignment, audio-visual SFT and MrDPO. LoRA is introduced during the audio-visual SFT stage. In each round of the MrDPO training, a new LoRA proxy is added while the old LoRA is merged into the LLM, so the model always contains only one activated LoRA.

3.3 Multi-round DPO

3.3.1 A Metric based on Atomic Events

We aim to leverage DPO to enhance the quality of video captions generated by the model. As for very detailed video captions, classical metrics such as BLEU and ROUGE-L are no longer able to measure the quality of the captions. To establish an effective evaluation method for caption completeness and accuracy, we propose using atomic events as an intermediary, enabling artificial intelligence (AI)-driven feedback to automatically assess and refine caption preferences. This approach guides the model toward generating more accurate and detailed video captions, ultimately achieving an automated RL training framework based on AI feedback.

Before DPO training, ground-truth video captions are first decomposed into atomic events using a powerful text LLM, such as GPT-4o, to provide references for evaluating the captions generated by the model. Next, we apply the nucleus sampling method [52] to generate caption pairs from the model’s output distribution for the input video.

The atomic events from the ground-truth video captions are used to identify the preferred sample within each pair. Specifically, we input a video caption and the corresponding list of ground-truth atomic events into a powerful text LLM like GPT-3.5. The LLM is prompted to identify which atomic events from the ground-truth list are missing in the caption, which events from the ground-truth list are described incorrectly, and which events described in the caption are absent from the ground-truth list. The missing ones are referred to as **“missing events”**, and the latter two types of events are referred to as **“hallucination events”**, respectively. The missing and hallucination rates for each caption are calculated by dividing the number of each type of event by the total number of atomic events in the ground-truth caption. The total error rate of a caption is then obtained by summing its missing and hallucination rates.

In each caption pair, the one with a lower total error rate is regarded as the preferred sample in DPO. To improve efficiency and mitigate the impact of LLM evaluation noise, caption pairs with small differences in these metrics are excluded from the DPO training set.

3.3.2 Multi-round DPO with LoRA Proxy

Unlike previous approaches that applied only single-round DPO to multimodal LLMs, we introduce a multi-round strategy, as prolonged offline training with a single round fails to optimise the model effectively due to the reference model being biased against the most recent model update in the DPO algorithm. In the multi-round framework, at each t th round, the following steps are taken to perform DPO training for the current round.

1. First, pre-trained LoRA module Δ_{t-1} is merged into the LLM backbone Λ_{t-1} to derive a new LLM backbone Λ_t that is equivalent to Λ_{t-1} with Δ_{t-1} , based on Eqn. (8):

$$\mathbf{W}_t = \mathbf{W}_{t-1} + \alpha \mathbf{A}_{t-1} \mathbf{B}_{t-1}, \quad (8)$$

where \mathbf{W}_t and \mathbf{W}_{t-1} are the weight parameters to adapt in Λ_t and Λ_{t-1} , α is the scaling factor of LoRA, r is the rank of LoRA, d is the dimension of \mathbf{W}_{t-1} . $\mathbf{A}_{t-1} \in \mathcal{R}^{d \times r}$ and $\mathbf{B}_{t-1} \in \mathcal{R}^{r \times d}$ are the low-rank matrix parameters of LoRA in the previous round $t-1$, and $\mathbf{W} \in \mathcal{R}^{d \times d}$ is the parameter of LLM backbone.

2. Next, a newly initialised LoRA module, $\tilde{\Delta}_t$, is added to the LLM backbone, forming the new policy model Λ_t for round t . During this round, only the LoRA parameters $\tilde{\Delta}_t$, referred to as the LoRA proxy, are updated, while all other LoRA parameters remain fixed. To mitigate the growing discrepancy between the reference and policy models caused by freezing the reference model in standard DPO, Λ_t is adopted as the updated reference model for round t .
3. At last, $\tilde{\Delta}_t$ is trained to obtain Δ_t , which can be achieved using the standard DPO loss. However, after multiple training rounds, the model is prone to getting stuck in local optima, leading to stagnant performance. To alleviate this issue by stabilising the training, a guided DPO (gDPO) loss is proposed as

$$\begin{aligned} \mathcal{L}_{\text{gDPO}}(\pi_\theta; \pi_{\text{ref}}) = & -\mathbb{E}_{(\mathbf{x}, \mathbf{y}_{\text{win}}, \mathbf{y}_{\text{lose}}) \sim \mathcal{D}} \left[\log \sigma \left(\beta \log \frac{\pi_\theta(\mathbf{y}_{\text{win}} \mid \mathbf{x})}{\pi_{\text{ref}}(\mathbf{y}_{\text{win}} \mid \mathbf{x})} - \beta \log \frac{\pi_\theta(\mathbf{y}_{\text{lose}} \mid \mathbf{x})}{\pi_{\text{ref}}(\mathbf{y}_{\text{lose}} \mid \mathbf{x})} \right) \right] \\ & + \lambda \mathbb{E}_{(\mathbf{x}, \mathbf{y}_{\text{gt}}) \sim \mathcal{D}_{\text{gt}}} \log \pi_\theta(\mathbf{y}_{\text{gt}} \mid \mathbf{x}), \end{aligned} \quad (9)$$

where $\pi_\theta = \{\Lambda_t, \tilde{\Delta}_t\}$ and $\pi_{\text{ref}} = \Lambda_t$ represent the policy and reference models for round t respectively, σ is the sigmoid function, and β is a hyper-parameter controlling the deviation from π_{ref} . Variables in the first term follow the definitions in the standard DPO loss [35]. In the second term corresponding to cross-entropy learning towards the ground-truth video captions, λ is the weight of the second term in the overall loss, \mathcal{D}_{gt} denotes the SFT training dataset, and $(\mathbf{x}, \mathbf{y}_{\text{gt}})$ corresponds to a video and its paired ground-truth text description. \mathbf{y}_{win} and \mathbf{y}_{lose} are preferred and dispreferred video captions generated by Λ_t for \mathbf{x} , which are judged using a text LLM based on the atomic-event-based metric proposed in Section 3.3.1. Each mini-batch of training samples is randomly selected from \mathcal{D}_{gt} .

4 Experimental Setup

4.1 Model Specifications

video-SALMONN 2 is built on an internally trained high-performance visual LLM, which is further fine-tuned on LLaVA-OneVision-7B [15]. The model processes video frames at a per-second frame rate of 1 (*i.e.*, $\phi = 1$), and can handle up to 110 frames. For videos longer than 110 seconds, 110 frames are uniformly sampled from the video.

For the audio branch, we use the Whisper-Large-v3 encoder [53] as the audio encoder, and a window-level Q-Former [54] with a window length of 0.5 seconds as the audio aligner, producing a total of 60 audio tokens for a 30-second input. The Whisper encoder has a maximum processing duration of $t_{\text{max}} = 30$ seconds. The rank r and scaling factor α of LoRA are set to 128 and 2.0, respectively. During training, the visual encoder, the audio encoder, and LLM remain frozen.

4.2 Data and Training Specifications

In the audio modality alignment stage, LibriSpeech-960h [55] and AudioCaps [56] are used to train the audio aligner. LibriSpeech-960h is utilized for speech recognition training, while AudioCaps is employed for audio captioning training. In the audio-visual SFT stage, experiments are performed

using about 13k videos with rich audio information from LLaVA-Video-178k [16] and FineVideo [57]. Both video captioning and video QA are trained during audio-visual SFT.

In the MrDPO stage, before each training round, the model generates a pair of captions for each video in the SFT dataset. To determine whether a caption pair is suitable for DPO, we evaluate the missing information rate and hallucination rate using GPT-3.5. It is also feasible to use a smaller model for evaluation, as shown in Appendix A. If deemed suitable, one caption is selected as the preferred sample, while the other is rejected. The selection criteria for each round are detailed in Appendix B. We use a learning rate of 2×10^{-5} in the first two DPO rounds, 1×10^{-5} for the third round, and 2×10^{-6} afterwards. We explore the values of λ in Eqn. (9) in Appendix C and finally set it to 0.1 throughout the entire MrDPO stage. Since only video captioning is trained during MrDPO, the video QA performance of the model will slightly decline. Therefore, SFT data for video QA will be added to the training process in the final round of MrDPO to enhance the video QA performance of the final model.

For the test dataset, we curated a video captioning benchmark to evaluate the event missing rate (Miss) and hallucination rate (Hall). Details of the test data can be found in Appendix D. The benchmark consists of 483 carefully selected videos, each labelled with complete audio-visual captions by human annotators. Atomic events for the test dataset were initially obtained using GPT-4o and then manually refined. The benchmark is open-sourced³. GPT-3.5 is used to evaluate the event missing and hallucination rates of the generated captions. Details are shown in Appendix E.

Regarding training settings, the resource consumption for each training step is shown in Table 1. In our experiments, we run a total of six gDPO rounds in MrDPO.

Table 1: Resource consumption in each training stage.

Training Stage	Used GPUs	Batch Size / GPU	Updates	Training Time
Audio Modality Alignment	$32 \times$ H800s	8	30,000	3 hours
Audio-Visual SFT	$32 \times$ H800s	1	15,475	14 hours
MrDPO Round 1-5	$8 \times$ H800s	1	1,000	2 hours
MrDPO Round 6	$32 \times$ H800s	1	841	1 hours

5 Experimental Results

5.1 Overall Results

The results of different models are presented in Table 2. In terms of video captioning, video-SALMONN 2 outperforms other models in both information missing and hallucination rates on our caption benchmark. Among existing open-source multimodal LLMs, few can provide detailed and accurate video descriptions, whether purely visual models like Qwen2.5-VL [17], InternVideo 2.5 [58] and VideоЛLaMA 3 [19], or audio-visual models like video-SALMONN [30], VideоЛLaMA 2 [29] and Qwen2.5-Omni [45]. The caption quality of Qwen2.5-VL is the best among open-source models. Notably, some open-source models, such as Video-LLaMA 3, tend to generate shorter captions, leading to relatively high information missing rates but low hallucination rates. Existing open-source audio-visual LLMs like video-SALMONN and VideоЛLaMA 2 fail to generate high-quality video captions. video-SALMONN has a very high total error rate, while VideоЛLaMA 2's captions are too short to contain all the details in the video. Qwen2.5-Omni can perceive both audio and visual information simultaneously, but still mainly focuses on visual information, often omitting human speech in audio and other sound events in captions. Among commercial models, GPT-4o and Gemini 1.5 Pro are capable of generating higher-quality and more detailed captions compared to current open-source models. However, the visual-only version of GPT-4o lacks audio comprehension, leading to a higher rate of missed events. Meanwhile, Gemini's understanding of visual content is somewhat limited, causing both models to exhibit varying degrees of information omission and hallucination.

Trained based on a visual base model with average performance, video-SALMONN 2 can ultimately achieve the SOTA performance in video captioning, even surpassing commercial models like GPT-4o and Gemini-1.5-Pro. On our caption benchmark, video-SALMONN 2 has reduced the event missing rate by more than 13%, the event hallucination rate by more than 14%, and the total error rate by nearly 28%, compared with the visual base model. The models' performance on our caption

³https://huggingface.co/datasets/videoSALMONN2/video-SALMONN_2_testset

benchmark is highly correlated with their performance on the "detailed" subset of the VDC caption benchmark [41], since both benchmarks evaluate the completeness of the model’s captions. In the VDC benchmark, which evaluates video captions from different perspectives, video-SALMONN 2 also achieves the SOTA results in the "detailed" subset among similar-size models, indicating the effectiveness of our training methods. We also perform Elo ranking with human evaluators inspired by [41], which validates the alignment of our proposed metrics with human perception and highlights the strong video captioning capabilities of video-SALMONN 2. Details are provided in Appendix F.

Besides, as an audio-visual LLM, video-SALMONN 2 retains strong visual understanding capabilities and performs well on various video benchmarks. In benchmarks like Video-MME [59], where audio information is taken into account in benchmark design, video-SALMONN 2 significantly outperforms the visual base model and is also superior to other open-source models. On purely visual benchmarks like NeXT-QA [60] and MLVU [61], video-SALMONN 2 also obtains competitive results.

Table 2: Results of our benchmark for video captioning evaluation. "A" and "V" refer to the audio and visual modalities, respectively. The event missing rate (Miss), hallucination rate (Hall), and total error rate (Total = Miss + Hall) are assessed for the captions. Results of some QA benchmarks like Video-MME (VMME), NeXT-QA (NQA) and MLVU are listed here as well.

Model	Modality	Our Caption Benchmark			VDC Detailed %Acc↑ Score↑	VMME %Acc↑	NQA %Acc↑	MLVU %Acc↑
		%Miss↓	%Hall↓	%Total↓				
GPT-4o Visual	V	17.0	14.2	31.2	46.3 2.5	71.9	-	-
Gemini-1.5-Pro	A + V	21.8	16.5	38.3	43.1 2.2	75.0	-	-
7B Qwen2.5-VL	V	21.9	17.4	39.2	44.5 2.4	65.1	-	70.2
7B InternVideo 2.5	V	30.8	15.0	45.8	39.6 2.2	65.1	-	72.8
7B VideoLLaMA 3	V	44.9	11.6	56.5	33.4 1.9	66.2	84.5	73.0
13B video-SALMONN	A + V	52.1	26.6	78.7	- -	43.3	49.2	-
7B VideoLLaMA 2	A + V	56.8	8.9	65.7	- -	54.9	75.6	-
7B Qwen2.5-Omni	A + V	26.3	21.7	48.1	39.7 2.2	64.3	82.9	68.3
7B Ours-Visual Base	V	23.3	27.4	50.7	42.2 2.3	62.9	83.6	69.2
7B video-SALMONN 2	A + V	10.0	12.9	22.9	46.1 2.5	67.4	83.0	68.0

5.2 Analysis of MrDPO

MrDPO is not just an iteration of round by round DPO, but also contains three key elements: updating to the DPO reference model periodically, using gDPO loss in Eqn. (9) instead of classical DPO loss, and continuously merging old LoRA and reinitialising new LoRA between rounds. During a single round of DPO training, the model converges after adequate steps of updates, for instance, approximately 1000 steps in our experiments. This is because the gap between the reference model and the policy model keeps increasing during training, which makes samples generated by the reference model can no longer guide the optimisation of the policy model. Therefore, it is necessary to periodically update the reference model to ensure continuous guidance from the positive-negative sample pairs generated by the reference model.

Due to the absence of supervised training with teacher forcing, DPO is conducted solely based on preference pairs, which can lead to instability during training. In particular, the DPO optimisation process is prone to getting trapped in local optima after several training rounds. To address this issue, we propose the gDPO loss, which incorporates an additional regularisation term based on ground-truth captions. This modification stabilises training, enabling more consistent optimisation during the MrDPO process. As shown in Fig.3a, while the classical DPO loss slightly outperforms gDPO in the first training round, gDPO demonstrates a clear advantage from the second round onward. This suggests that the cross-entropy term introduced in Eqn. (9) plays a critical role in improving training stability.

As shown in Fig. 3b, continuously merging and reinitialising the LoRA proxy in each DPO round leads to improved MrDPO performance, particularly during the early stages, compared to reusing a fixed LoRA proxy. This improvement likely stems from two factors: merging the previous LoRA into the LLM progressively strengthens the model’s foundation by integrating prior adaptations, while initialising a new LoRA in each round allows the model to explore fresh low-rank subspaces aligned with current preference signals. In the initial rounds, when the model has not yet been fine-tuned for preference-specific behaviours, a newly initialised LoRA proxy helps avoid stagnation in outdated

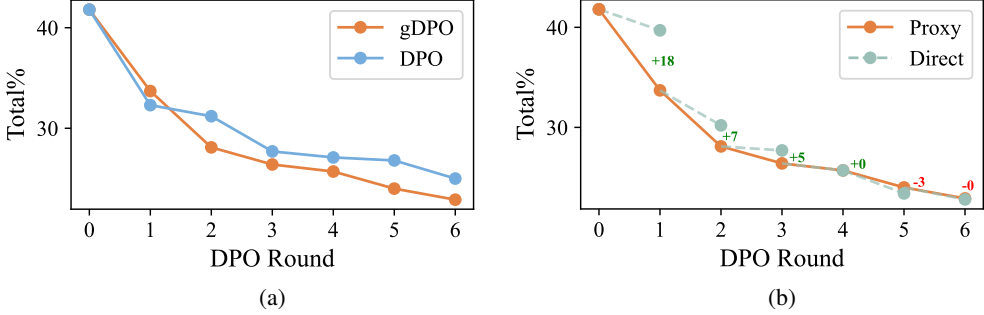


Figure 3: SubFig. (a) compares the performances of training with the proposed gDPO loss and the classical DPO loss for six rounds, denoted as “gDPO” and “DPO”. SubFig. (b) compares the performance between training a new LoRA proxy in each round and directly fine-tuning the existing LoRA based on the model of the last MrDPO round, denoted as “Proxy” and “Direct”. Total error rates on our caption benchmark are evaluated here.

parameter subspaces, enabling more flexible learning of core reward structures. In contrast, retraining the same LoRA proxy restricts updates to subspaces optimised for earlier data, limiting the model’s adaptability to evolving signals. The advantage of this strategy diminishes in later rounds, as the merged LLM gradually accumulates prior improvements, and the marginal benefit of introducing a new LoRA becomes less significant.

5.3 Answering Video QA Based on Video Captions

Another way to evaluate caption completeness is by using the generated video captions rather than the raw video frames as input to a powerful text-based LLM for the video QA task. We used the Video-MME benchmark [59] for test. Specifically, we first use captioning models to generate descriptions for each video in Video-MME, and then prompt GPT-4o to answer the relevant questions based solely on these captions. In this setting, higher QA accuracy suggests that the generated captions are more complete and informative. We report the performance of various models under this evaluation protocol in Table 3.

In this manner, using video-SALMONN 2 captions achieves the highest accuracy, even surpassing the QA accuracy by GPT-4o itself, which indicates that video-SALMONN 2’s captions are complete enough to provide clues for video QA. Furthermore, the results in Table 3 are highly correlated with the performance of the models on our caption benchmark in Table 2, since both evaluation methods require video captions to be detailed and accurate. This also validates the soundness of the caption metrics we proposed.

6 Limitations

Although video-SALMONN 2 has significantly improved the performance in video captioning, its performance in video QA does not improve compared to the visual base model, since we have not optimized video QA in this work. Besides, this somehow indicates that video captioning and video QA may involve different capabilities of multimodal LLMs. Improving one of them does not necessarily lead to an improvement in the other. This issue is not explored in depth in this work and will be investigated in our future research.

7 Conclusions

This work presents video-SALMONN 2, a powerful audio-visual LLM designed for detailed video captioning, along with the MrDPO method. To our knowledge, this is the first study to apply RL for video captioning to multimodal LLMs in the literature. We introduce new metrics to evaluate missing information and hallucination rates in video captions, which guide sample selection for DPO. To enhance training stability and the final performance, we incorporate a novel gDPO loss with LoRA proxy in MrDPO. As a result, video-SALMONN 2 achieves substantial improvements in video captioning, surpassing proprietary leading models such as GPT-4o and Gemini-1.5-Pro, paving the way for more detailed and accurate video understanding.

Table 3: QA results of GPT-4o on Video-MME based on video descriptions generated by the captioning models.

Captioning Model	%Acc↑
GPT-4o	64.3
Qwen2.5-VL	55.0
InternVideo 2.5	51.8
VideoLLaMA 3	46.3
Qwen2.5-Omni	52.7
video-SALMONN 2	65.9

References

- [1] OpenAI, Josh Achiam, Steven Adler, Sandhini Agarwal, Lama Ahmad, et al. GPT-4 Technical Report, 2024.
- [2] Abhimanyu Dubey, Abhinav Jauhri, Abhinav Pandey, Abhishek Kadian, Ahmad Al-Dahle, Aiesha Letman, Akhil Mathur, Alan Schelten, et al. The LLaMA 3 Herd of Models. *arXiv preprint arXiv:2407.21783*, 2024.
- [3] Hugo Touvron, Thibaut Lavril, Gautier Izacard, Xavier Martinet, Marie-Anne Lachaux, et al. LLaMA: Open and Efficient Foundation Language Models. *arXiv preprint arXiv:2302.13971*, 2023.
- [4] Zhengxiao Du, Yujie Qian, Xiao Liu, Ming Ding, Jiezhong Qiu, Zhilin Yang, and Jie Tang. GLM: General Language Model Pretraining with Autoregressive Blank Infilling. In *Proc. ACL*, Dublin, 2022.
- [5] An Yang, Anfeng Li, Baosong Yang, Beichen Zhang, et al. Qwen3 Technical Report. *arXiv preprint arXiv:2505.09388*, 2025.
- [6] Daya Guo, Dejian Yang, Haowei Zhang, Junxiao Song, Ruoyu Zhang, Runxin Xu, Qihao Zhu, Shirong Ma, Peiyi Wang, Xiao Bi, et al. DeepSeek-R1: Incentivizing Reasoning Capability in LLMs via Reinforcement Learning. *arXiv preprint arXiv:2501.12948*, 2025.
- [7] Haotian Liu, Chunyuan Li, Qingyang Wu, and Yong Jae Lee. Visual Instruction Tuning. In *Proc. NeurIPS*, Vancouver, 2024.
- [8] Haotian Liu, Chunyuan Li, Yuheng Li, and Yong Jae Lee. Improved Baselines with Visual Instruction Tuning. In *Proc. CVPR*, Seattle, 2024.
- [9] Junnan Li, Dongxu Li, Silvio Savarese, and Steven Hoi. BLIP-2: Bootstrapping Language-Image Pre-training with Frozen Image Encoders and Large Language Models. In *Proc. ICML*, 2023.
- [10] Jinze Bai, Shuai Bai, Shusheng Yang, Shijie Wang, Sinan Tan, Peng Wang, Junyang Lin, Chang Zhou, and Jingren Zhou. Qwen-VL: A Versatile Vision-Language Model for Understanding, Localization, Text Reading, and Beyond. *arXiv preprint arXiv:2308.12966*, 2023.
- [11] Ji Lin, Hongxu Yin, Wei Ping, Yao Lu, Pavlo Molchanov, Andrew Tao, Huizi Mao, Jan Kautz, Mohammad Shoeybi, and Song Han. VILA: On Pre-training for Visual Language Models. *arXiv preprint arXiv:2312.07533*, 2023.
- [12] Zhe Chen, Jiannan Wu, Wenhui Wang, Weijie Su, Guo Chen, Sen Xing, Muyan Zhong, Qinglong Zhang, Xizhou Zhu, Lewei Lu, Bin Li, Ping Luo, Tong Lu, Yu Qiao, and Jifeng Dai. InternVL: Scaling up Vision Foundation Models and Aligning for Generic Visual-Linguistic Tasks. *arXiv preprint arXiv:2312.14238*, 2023.
- [13] Bin Lin, Bin Zhu, Yang Ye, Munan Ning, Peng Jin, and Li Yuan. Video-LLaVA: Learning United Visual Representation by Alignment Before Projection. In *Proc. CVPR*, Seattle, 2024.
- [14] Lin Chen, Xilin Wei, Jinsong Li, Xiaoyi Dong, Pan Zhang, Yuhang Zang, Zehui Chen, Haodong Duan, Bin Lin, Zhenyu Tang, et al. ShareGPT4Video: Improving Video Understanding and Generation with Better Captions. *arXiv preprint arXiv:2406.04325*, 2024.
- [15] Bo Li, Yuanhan Zhang, Dong Guo, Renrui Zhang, Feng Li, Hao Zhang, Kaichen Zhang, Peiyuan Zhang, Yanwei Li, Ziwei Liu, et al. Llava-OneVision: Easy visual task transfer. *arXiv preprint arXiv:2408.03326*, 2024.
- [16] Yuanhan Zhang, Jinming Wu, Wei Li, Bo Li, Zejun Ma, Ziwei Liu, and Chunyuan Li. Video Instruction Tuning with Synthetic Data. *arXiv preprint arXiv:2410.02713*, 2024.
- [17] Shuai Bai, Keqin Chen, Xuejing Liu, Jialin Wang, Wenbin Ge, Sibo Song, Kai Dang, Peng Wang, Shijie Wang, Jun Tang, et al. Qwen2.5-VL Technical Report. *arXiv preprint arXiv:2502.13923*, 2025.
- [18] Yixuan Li, Changli Tang, Jimin Zhuang, Yudong Yang, Guangzhi Sun, Wei Li, Zejun Ma, and Chao Zhang. Improving LLM Video Understanding with 16 Frames Per Second. *arXiv preprint arXiv:2503.13956*, 2025.
- [19] Boqiang Zhang, Kehan Li, Zesen Cheng, Zhiqiang Hu, Yuqian Yuan, Guanzheng Chen, Sicong Leng, Yuming Jiang, Hang Zhang, Xin Li, et al. VideoLLaMA 3: Frontier Multimodal Foundation Models for Image and Video Understanding. *arXiv preprint arXiv:2501.13106*, 2025.

[20] Jian Wu, Yashesh Gaur, Zhuo Chen, Long Zhou, Yimeng Zhu, Tianrui Wang, Jinyu Li, Shujie Liu, Bo Ren, Linquan Liu, et al. On Decoder-only Architecture for Speech-to-Text and Large Language Model Integration. In *Proc. ASRU*, Taipei, 2023. IEEE.

[21] Changli Tang, Wenyi Yu, Guangzhi Sun, Xianzhao Chen, Tian Tan, Wei Li, Lu Lu, Zejun MA, and Chao Zhang. SALMONN: Towards Generic Hearing Abilities for Large Language Models. In *Proc. ICLR*, Vienna, 2024.

[22] Yunfei Chu, Jin Xu, Xiaohuan Zhou, Qian Yang, Shiliang Zhang, Zijie Yan, Chang Zhou, and Jingren Zhou. Qwen-Audio: Advancing Universal Audio Understanding via Unified Large-Scale Audio-Language Models. *arXiv preprint arXiv:2311.07919*, 2023.

[23] Yunfei Chu, Jin Xu, Qian Yang, Haojie Wei, Xipin Wei, Zhifang Guo, Yichong Leng, Yuanjun Lv, Jinzheng He, Junyang Lin, Chang Zhou, and Jingren Zhou. Qwen2-Audio Technical Report. *arXiv preprint arXiv:2407.10759*, 2024.

[24] Yuan Gong, Hongyin Luo, Alexander H. Liu, Leonid Karlinsky, and James R. Glass. Listen, Think, and Understand. In *Proc. ICLR*, Vienna, 2024.

[25] Yuan Gong, Alexander H. Liu, Hongyin Luo, Leonid Karlinsky, and James Glass. Joint Audio and Speech Understanding. In *Proc. ASRU*, Taipei, 2023.

[26] Changli Tang, Wenyi Yu, Guangzhi Sun, Xianzhao Chen, Tian Tan, Wei Li, Jun Zhang, Lu Lu, Zejun Ma, Yuxuan Wang, and Chao Zhang. Can Large Language Models Understand Spatial Audio. In *Interspeech 2024*, Kos Island, 2024.

[27] Zhisheng Zheng, Puyuan Peng, Ziyang Ma, Xie Chen, Eunsol Choi, and David Harwath. BAT: Learning to Reason about Spatial Sounds with Large Language Models. In *Proc. ICML*, 2024.

[28] Gemini Team, Rohan Anil, Sebastian Borgeaud, Jean-Baptiste Alayrac, Jiahui Yu, et al. Gemini: A Family of Highly Capable Multimodal Models. *arXiv preprint arXiv:2312.11805*, 2024.

[29] Zesen Cheng, Sicong Leng, Hang Zhang, Yifei Xin, Xin Li, Guanzheng Chen, Yongxin Zhu, Wenqi Zhang, Ziyang Luo, Deli Zhao, and Lidong Bing. VideoLLaMA 2: Advancing Spatial-Temporal Modeling and Audio Understanding in Video-LLMs. *arXiv preprint arXiv:2406.07476*, 2024.

[30] Guangzhi Sun, Wenyi Yu, Changli Tang, Xianzhao Chen, Tian Tan, Wei Li, Lu Lu, Zejun MA, Yuxuan Wang, and Chao Zhang. video-SALMONN: Speech-Enhanced Audio-Visual Large Language Models. In *Proc. ICML*, 2024.

[31] Chaoyou Fu, Haojia Lin, Zuwei Long, Yunhang Shen, Meng Zhao, Yifan Zhang, Xiong Wang, Di Yin, Long Ma, Xiawu Zheng, Ran He, Rongrong Ji, Yunsheng Wu, Caifeng Shan, and Xing Sun. VITA: Towards Open-Source Interactive Omni Multimodal LLM. *arXiv preprint arXiv:2408.05211*, 2024.

[32] Chaoyou Fu, Haojia Lin, Xiong Wang, Yi-Fan Zhang, Yunhang Shen, Xiaoyu Liu, Haoyu Cao, Zuwei Long, Heting Gao, Ke Li, et al. VITA-1.5: Towards GPT-4o Level Real-Time Vision and Speech Interaction. *arXiv preprint arXiv:2501.01957*, 2025.

[33] Yunlong Tang, Daiki Shimada, Jing Bi, and Chenliang Xu. AVicuna: Audio-visual LLM with Interleaver and Context-Boundary Alignment for Temporal Referential Dialogue. *arXiv preprint arXiv:2403.16276*, 2024.

[34] Guangzhi Sun, Yudong Yang, Jimin Zhuang, Changli Tang, Yixuan Li, Wei Li, Zejun MA, and Chao Zhang. video-SALMONN-01: Reasoning-enhanced Audio-visual Large Language Model. *arXiv preprint arXiv:2502.11775*, 2025.

[35] Rafael Rafailov, Archit Sharma, Eric Mitchell, Christopher D Manning, Stefano Ermon, and Chelsea Finn. Direct Preference Optimization: Your Language Model is Secretly a Reward Model. In *Proc. NeurIPS*, Vancouver, 2024.

[36] Edward J. Hu, Yelong Shen, Phillip Wallis, Zeyuan Allen-Zhu, Yuanzhi Li, Shean Wang, Lu Wang, and Weizhu Chen. LoRA: Low-Rank Adaptation of Large Language Models. In *Proc. ICLR*, 2022.

[37] Jason Wei, Maarten Bosma, Vincent Zhao, Kelvin Guu, Adams Wei Yu, Brian Lester, Nan Du, Andrew M Dai, and Quoc V Le. Finetuned Language Models are Zero-Shot Learners. In *Proc. ICML*, 2022.

[38] Ruohong Zhang, Liangke Gui, Zhiqing Sun, Yihao Feng, Keyang Xu, Yuanhan Zhang, Di Fu, Chunyuan Li, Alexander Hauptmann, Yonatan Bisk, and Yiming Yang. Direct Preference Optimization of Video Large Multimodal Models from Language Model Reward. *arXiv preprint arXiv:2404.01258*, 2024.

[39] Peng Wang, Shuai Bai, Sinan Tan, Shijie Wang, Zhihao Fan, Jinze Bai, Keqin Chen, Xuejing Liu, Jialin Wang, Wenbin Ge, et al. Qwen2-VL: Enhancing Vision-language Model’s Perception of The World at Any Resolution. *arXiv preprint arXiv:2409.12191*, 2024.

[40] Zhijian Liu, Ligeng Zhu, Baifeng Shi, Zhuoyang Zhang, Yuming Lou, Shang Yang, Haocheng Xi, Shiyi Cao, Yuxian Gu, Dacheng Li, et al. NVILA: Efficient Frontier Visual Language Models. *arXiv preprint arXiv:2412.04468*, 2024.

[41] Wenhao Chai, Enxin Song, Yilun Du, Chenlin Meng, Vashisht Madhavan, Omer Bar-Tal, Jenq-Neng Hwang, Saining Xie, and Christopher D Manning. Auroracap: Efficient, performant video detailed captioning and a new benchmark. *arXiv preprint arXiv:2410.03051*, 2024.

[42] Antoine Yang, Arsha Nagrani, Paul Hongsuck Seo, Antoine Miech, Jordi Pont-Tuset, Ivan Laptev, Josef Sivic, and Cordelia Schmid. Vid2seq: Large-scale Pretraining of a Visual Language Model for Dense Video Captioning. In *Proc. CVPR*, Vancouver, 2023.

[43] Hang Zhang, Xin Li, and Lidong Bing. Video-LLaMA: An Instruction-tuned Audio-Visual Language Model for Video Understanding. In *Proc. EMNLP: System Demonstrations*, Singapore, 2023.

[44] Yi Wang, Kunchang Li, Xinhao Li, Jiahuo Yu, Yinan He, Guo Chen, Baoqi Pei, Rongkun Zheng, Jilan Xu, Zun Wang, et al. Internvideo2: Scaling Video Foundation Models for Multimodal Video Understanding. *arXiv preprint arXiv:2403.15377*, 2024.

[45] Jin Xu, Zhifang Guo, Jinzheng He, Hangrui Hu, Ting He, Shuai Bai, Keqin Chen, Jialin Wang, Yang Fan, Kai Dang, et al. Qwen2.5-Omni Technical Report. *arXiv preprint arXiv:2503.20215*, 2025.

[46] Long Ouyang, Jeffrey Wu, Xu Jiang, Diogo Almeida, Carroll Wainwright, Pamela Mishkin, Chong Zhang, Sandhini Agarwal, Katarina Slama, Alex Ray, et al. Training Language Models to Follow Instructions with Human Feedback. In *Proc. NeurIPS*, New Orleans, 2022.

[47] John Schulman, Filip Wolski, Prafulla Dhariwal, Alec Radford, and Oleg Klimov. Proximal Policy Optimization Algorithms. *arXiv preprint arXiv:1707.06347*, 2017.

[48] Kawin Ethayarajh, Winnie Xu, Niklas Muennighoff, Dan Jurafsky, and Douwe Kiela. KTO: Model Alignment as Prospect Theoretic Optimization. *arXiv preprint arXiv:2402.01306*, 2024.

[49] Harrison Lee, Samrat Phatale, Hassan Mansoor, Thomas Mesnard, Johan Ferret, Kellie Lu, Colton Bishop, Ethan Hall, Victor Carbune, Abhinav Rastogi, et al. RLAIF: Scaling Reinforcement Learning from Human Feedback with AI Feedback. *arXiv preprint arXiv:2309.00267*, 2023.

[50] Zhihong Shao, Peiyi Wang, Qihao Zhu, Runxin Xu, Junxiao Song, Xiao Bi, Haowei Zhang, Mingchuan Zhang, YK Li, Y Wu, et al. DeepSeekMath: Pushing the Limits of Mathematical Reasoning in Open Language Models. *arXiv preprint arXiv:2402.03300*, 2024.

[51] Wenyi Yu, Changli Tang, Guangzhi Sun, Xianzhao Chen, Tian Tan, Wei Li, Lu Lu, Zejun Ma, and Chao Zhang. Connecting Speech Encoder and Large Language Model for ASR. In *Proc. ICASSP*, Seoul, 2024.

[52] Ari Holtzman, Jan Buys, Li Du, Maxwell Forbes, and Yejin Choi. The Curious Case of Neural Text Degeneration. In *Proc. ICLR*, 2020.

[53] Alec Radford, Jong Wook Kim, Tao Xu, Greg Brockman, Christine McLeavy, and Ilya Sutskever. Robust Speech Recognition via Large-scale Weak Supervision. In *Proc. ICML*, 2023.

[54] Changli Tang, Wenyi Yu, Guangzhi Sun, Xianzhao Chen, Tian Tan, Wei Li, Lu Lu, Zejun Ma, and Chao Zhang. Extending Large Language Models for Speech and Audio Captioning. In *Proc. ICASSP*, Seoul, 2024.

[55] Vassil Panayotov, Guoguo Chen, Daniel Povey, and Sanjeev Khudanpur. Librispeech: An ASR corpus based on public domain audio books. In *Proc. ICASSP*, Brisbane, 2015.

[56] Chris Dongjoo Kim, Byeongchang Kim, Hyunmin Lee, and Gunhee Kim. AudioCaps: Generating Captions for Audios in The Wild. In *Proc. NAACL-HLT*, Minneapolis, 2019.

[57] Miquel Farré, Andi Marafioti, Lewis Tunstall, Leandro Von Werra, and Thomas Wolf. Finevideo. <https://huggingface.co/datasets/HuggingFaceFV/finevideo>, 2024.

[58] Yi Wang, Xinhao Li, Ziang Yan, Yinan He, Jiahuo Yu, Xiangyu Zeng, Chenting Wang, Changlian Ma, Haian Huang, Jianfei Gao, et al. InternVideo2.5: Empowering Video MLLMs with Long and Rich Context Modeling. *arXiv preprint arXiv:2501.12386*, 2025.

[59] Chaoyou Fu, Yuhang Dai, Yondong Luo, Lei Li, Shuhuai Ren, Renrui Zhang, Zihan Wang, Chenyu Zhou, Yunhang Shen, Mengdan Zhang, et al. Video-MME: The First-Ever Comprehensive Evaluation Benchmark of Multi-modal LLMs in Video Analysis. *arXiv preprint arXiv:2405.21075*, 2024.

[60] Junbin Xiao, Xindi Shang, Angela Yao, and Tat-Seng Chua. NExT-QA: Next Phase of Question-Answering to Explaining Temporal Actions. In *Proc. CVPR*, 2021.

[61] Junjie Zhou, Yan Shu, Bo Zhao, Boya Wu, Shitao Xiao, Xi Yang, Yongping Xiong, Bo Zhang, Tiejun Huang, and Zheng Liu. MLVU: A Comprehensive Benchmark for Multi-task Long Video Understanding. *arXiv preprint arXiv:2406.04264*, 2024.

A Training with Models with Smaller Scale as Evaluator

We also try using Qwen3-4B [5] as the LLM for evaluating the quality of video captions during training, and still use GPT-3.5 for testing. All prompts, generation settings, and training settings remain the same with the GPT-3.5 version. The results of using these two models as evaluators are similar, as shown in Table 4.

Table 4: The captioning results of using Qwen3-4B and GPT-3.5 as evaluators in the first gDPO round.

Evaluation LLM during training	Miss% \downarrow	Hall% \downarrow	Total% \downarrow
GPT-3.5	13.8	19.9	33.7
Qwen3-4B	14.3	19.4	33.7

B Samples Selecting Criteria in MrDPO

To achieve better performance and training efficiency, we take a specially designed strategy to select proper preference pairs. A sample pair is selected if one sample is significantly better than the other. We consider the total error rate Δe as the main metric. Besides, to avoid repeatedly decoding, we also consider the repetition rate Δr of each sample. Table 5 shows the threshold used in each round of MrDPO.

Table 5: The data selecting threshold used in each gDPO round. A negative number means that the chosen sample can be worse than the rejected sample in this metric to some degree.

gDPO Round	Threshold Used	
	Δe	Δr
1	$\geq 5\%$	$\geq 1\%$
2	$\geq 20\%$	$\geq -1\%$
3	$\geq 23\%$	$\geq -1\%$
4	$\geq 23\%$	$\geq -1\%$
5	$\geq 23\%$	$\geq -1\%$
6	$\geq 23\%$	$\geq -1\%$

C Hyperparameter Search in gDPO

In gDPO, the weight λ of the cross-entropy regularization term is an important hyperparameter. We simply performed a search over its values in the first round of MrDPO. Results are shown in Table 6.

As the results show, when λ is greater than 1, the weight of the cross entropy loss becomes too large and hinders the optimization of the DPO loss. On the other hand, although the model trained with small λ (less than 0.01) seems better in the first gDPO round, the cross-entropy term is too small to stabilise MrDPO training, as Figure 3a shows. Therefore, we finally choose 0.1 as a suitable value of λ .

Table 6: Results of the first round of MrDPO training with different λ .

λ	Our Caption Benchmark		
	%Miss \downarrow	%Hall \downarrow	%Total \downarrow
0	13.7	18.6	32.3
0.01	13.7	19.0	32.8
0.1	13.8	19.9	33.7
1	15.4	21.9	36.2
10	16.8	22.8	39.7

D About The Test Dataset

Figure 4 shows the video type distribution and the video length distribution of our caption benchmark. The benchmark covers 14 different fields. All the videos are between 30s to 60s, with an average duration of 51s. Table 7 shows more statistics about the labelled captions and atomic events of the benchmark. Specifically, there are 6.1 audio-related atomic events per video, including 4.6 speech-related events and 1.5 non-speech events.

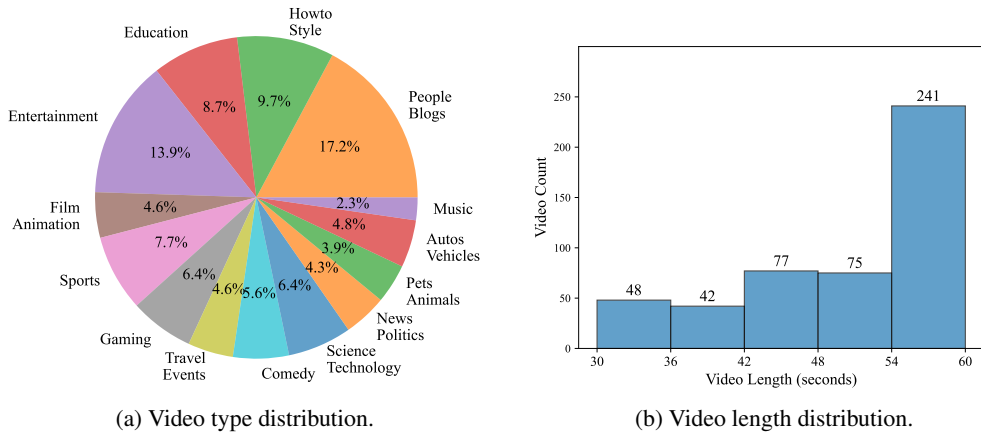


Figure 4: The basic information of our benchmark data.

Table 7: Statistics about the labelled captions and atomic events of the benchmark.

#Sample	#Vocabulary	#Word	Average Statistics	
			Caption Length	#Atomic Event
483	17137	296,938	615 words	34.2

E Evaluation Process on Our Caption Benchmark

During testing, GPT-3.5 is used as LLM for evaluating the quality of video captions. We input the captions generated by the model and the list of groundtruth atomic events into GPT-3.5, and ask GPT-3.5 to list the following three types of events and provide the quantity of each:

- Missing Events:** Atomic events from the ground-truth list that are missing in the caption.
- Incorrect Events:** Atomic events from the ground-truth list that are described incorrectly in the caption.
- Hallucination Events:** Events described in the caption that are absent from the ground-truth atomic event list.

Note that incorrect events and hallucination events both belong to the model’s “hallucination” and will be used to calculate the hallucination rate.

The quotient between the number of missing events and the number of all atomic events is the missing rate, and the quotient between the number of incorrect and hallucination events and the number of all atomic events is the hallucination rate. The total error rate is the sum of the missing and hallucination rates.

The prompts for testing can be referenced from the scripts provided in the [open-source test data](#).

F Elo Ranking Results

We perform the Elo ranking by human to rate the video captioning capability of Gemini-1.5-pro, GPT-4o, our visual base model, and the final video-SALMONN 2. Parameters of the Elo ranking system are provided in Table 8.

Table 8: Parameters of the Elo ranking system.

Parameter	Value
Initial ELO mean	1000
Base of logarithm	10
Scaling factor	400
K-factor	8

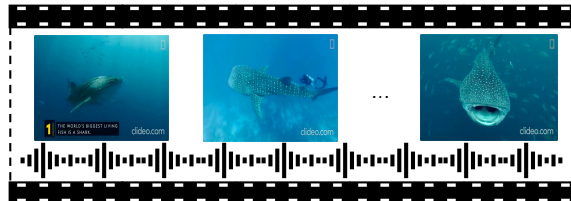
We collected 180 pairs of captions generated by different models as simulated matches. Annotators are provided with the video and two corresponding video captions generated by two different models, respectively, and they are expected to select the better caption according to the completeness and correctness of the caption. The final Elo rating results and the total error rates on our benchmark of each model are provided in Table 9.

Table 9: Elo rating results compared with the total error rates of different models. “Total” represents the total error rate of video captioning on our caption benchmark.

Model	Total%↓	Elo Rating↑
GPT-4o Visual	31.2	976
Gemini-1.5-pro	38.3	964
Ours-Visual Base	50.7	945
video-SALMONN 2	22.9	1115

G An Example of Atomic Events

We show an example of atomic events of a randomly selected video in Fig. 5.



Atomic Event List

1. The video begins with a whale shark swimming in the ocean.
2. The whale shark moves slowly through the water.
3. The number '1' in a yellow box appears in the video.
4. The text 'THE WORLD'S BIGGEST LIVING FISH IS A SHARK.' appears in the video.
5. A vibrant coral reef teeming with small fish appears.
6. A woman says, "The world's biggest living fish is a shark. Of the estimated 34,000 species of fish, the largest are whale sharks."
7. Background music can be heard.
8. A diver swims near the whale shark.
9. The scene changes again, showing a diver swimming near the whale shark.
10. A woman's voice says, "These gentle giants usually grow to about 40 feet long and weigh an estimated 15 tons. Their mouths alone can span 4 feet wide."
11. The background music continues.
12. Text 'clideo.com' can be seen in the bottom right corner.
13. The scene changes, showing a close-up view of the whale shark's mouth.

Figure 5: An example of the atomic event list of a video.